

Molecular docking studies on 4-thiazolidinones as HIV-1 RT inhibitors

Ravindra K. Rawal · Ashutosh Kumar ·
Mohammad Imran Siddiqi · Setu B. Katti

Received: 26 April 2006 / Accepted: 6 July 2006 / Published online: 13 September 2006
© Springer-Verlag 2006

Abstract Flexible docking simulations were performed on two series of 4-thiazolidinones as HIV-1 reverse transcriptase (HIV-1 RT) inhibitors. This was done by analyzing the interaction of these compounds with the allosteric site of the HIV-1 reverse transcriptase enzyme. The binding scores for these compounds were also congruent with their anti-HIV activity. A good correlation between the predicted binding free energies and the experimentally observed inhibitory activities (EC_{50}) suggest that the identified binding conformations of these inhibitors are reliable. The results of docking studies provide an insight into the pharmacophoric structural requirements for the HIV-1 RT inhibitory activity of this class of molecules.

Keywords HIV-1 RT inhibitors · 4-thiazolidinone · Molecular docking

Introduction

During the past decade, there has been steady progress in the chemotherapy of AIDS due to the availability of more effective antiretroviral drugs [1]. All clinically used antiretroviral drugs belong to either the protease inhibitor (PI) or reverse transcriptase inhibitor (NRTIs) classes. There are at least five drugs in clinical use from the latter class. Non-

nucleoside reverse transcriptase (NNRTIs) inhibitors have attracted special status as drug candidates because of their unique mode of action, non-covalent, and non competitive binding at the allosteric site, which is present only in the HIV-1 RT [2]. However, this scenario is changing due to the emergence of drug resistant HIV-variants. Therefore, a better understanding of drug-HIV-1 RT interactions at the molecular level has become essential. It is hoped that this knowledge will provide valuable information in designing NNRTIs with a broad spectrum of activity.

A number of computational approaches are currently used to obtain deeper insight into the drug, enzyme interactions. Recently, the 2,3-diaryl-thiazolidin-4-one scaffold has emerged from Pietro Monforte's group as a selective NNRTI [3, 4]. QSAR and modeling studies on the HIV-1 RT inhibitory activity of 2,3-diaryl-thiazolidin-4-ones by our group and others indicated the importance of overall hydrophobicity of the analogues, and steric and electronic features of meta/para substitution of the 3-aryl moiety [5–7]. They also suggested that a heteroaryl system would be preferred over the 3-aryl moiety for better HIV-1 RT inhibitory activity [8, 9]. As a logical extension of our earlier work, we have carried out a molecular docking on this series of compounds. The results from this study should be useful in understanding the inhibitory mode of the 4-thiazolidinones and in designing new drug leads against HIV-1 RT.

R. K. Rawal · S. B. Katti (✉)
Medicinal and Process Chemistry Division,
Central Drug Research Institute,
Lucknow 226001, India
e-mail: setu_katti@yahoo.com

A. Kumar · M. I. Siddiqi
Division of Molecular & Structural Biology,
Central Drug Research Institute,
Lucknow 226001, India

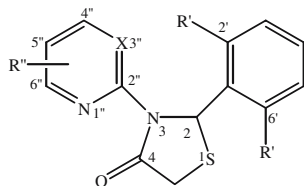
Computational methods

Molecular structures and optimization

The biological activity data of 2,3-diaryl-1,3-thiazolidin-4-ones (38 molecules), reported by Monforte et al. [3, 4] is

used in the present study (Table 1). The structures of all compounds reported in Table 1 were constructed using the InsightII Builder module [10]. The geometries of these compounds were subsequently optimized by Sybyl 7.0

Table 1 2-(2,6-Dihalophenyl)-3-(substituted heteroaryl)-thiazolidin-4-ones and their HIV-1 RT inhibitory activity



Comp no.	X	R''			R'	Obs. value ($-\log EC_{50}$)
		4''	5''	6''		
Pyridine analogues						
1	CH	H	H	H	Cl Cl	6.75
2	CH	H	H	H	Cl F	6.56
3	CH	H	H	H	F F	6.07
4	CH	H	Cl	H	Cl Cl	5.75
5	CH	H	Cl	H	Cl F	5.67
6	CH	H	Cl	H	F F	5.14
7	CH	H	Br	H	Cl Cl	5.82
8	CH	H	Br	H	Cl F	5.91
9	CH	H	Br	H	F F	5.31
10	CH	H	H	Br	Cl Cl	6.56
11	CH	H	H	Br	Cl F	7.19
12	CH	H	H	Br	F F	7.52
13 ^a	CH ₃	H	H	H	F F	4.27
14	CH	CH ₃	H	H	Cl Cl	6.83
15	CH	CH ₃	H	H	Cl F	7.00
16	CH	CH ₃	H	H	F F	6.60
17	CH	H	CH ₃	H	Cl Cl	5.85
18	CH	H	CH ₃	H	F F	5.29
19	CH	H	H	CH ₃	Cl Cl	7.36
20	CH	H	H	CH ₃	Cl F	7.28
21	CH	H	H	CH ₃	F F	7.09
22	CH	CH ₃	H	CH ₃	Cl Cl	7.04
23	CH	CH ₃	H	CH ₃	Cl F	7.38
24	CH	CH ₃	H	CH ₃	F F	7.23
Pyrimidine analogues						
25	N	H	H	H	Cl Cl	6.64
26	N	H	H	H	Cl F	6.24
27	N	H	H	H	F F	5.44
28	N	CH ₃	H	H	Cl Cl	7.36
29	N	CH ₃	H	H	Cl F	7.13
30	N	CH ₃	H	H	F F	6.41
31	N	CH ₃	H	Cl	Cl Cl	4.29
32	N	CH ₃	H	CH ₃	Cl Cl	7.77
33	N	CH ₃	H	CH ₃	Cl F	7.42
34	N	CH ₃	H	CH ₃	F F	6.77
35	N	CH ₃	H	CH ₃ O	Cl Cl	7.62
36	N	CH ₃	H	CH ₃ O	Cl F	7.25
37	N	CH ₃	H	CH ₃ O	F F	6.58
38	N	CH ₃	H	OH	Cl Cl	4.48

[11] using the Tripos force field and Gasteiger–Huckel charges [12]. The Powell method was used for energy minimization with an energy convergence gradient of 0.001 kcal mol⁻¹. The structure of HIV-1 RT protein (PDB code 1REV) was obtained from Protein Data Bank [Research Collaboratory for Structural Bioinformatics (RCSB)] (<http://www.rcsb.org/pdb>). Kollman united-atom charges were assigned to protein atoms using Sybyl 7.0.

Docking simulations

Docking simulations were carried out using the FlexX program [13] interfaced with SYBYL 7.0. FlexX is a fast algorithm for the flexible docking of small ligands into fixed protein binding sites using an incremental construction process [14, 15]. Based on previously reported structural information, the active-site regions for the comparative FlexX docking simulations of 4-thiazolidinones with HIV-1 RT were constructed [16–18]. The proposed interaction modes of the ligand with the HIV-1 RT binding site were determined as the highest scored conformation (best-fit ligand) among the 30 conformations. The binding modes were generated according to the FlexX scoring (Table 2), which was represented by the structure with the most favorable binding free energy (ΔG_{bind}). FlexX uses a purely empirical scoring function similar to that developed by Rarey et al. [14] and Böhm [19]. The binding free energy of a protein/ligand complex was estimated as the sum of the free energy contributions from hydrogen bonding, ion-pair interactions, hydrophobic and π -stacking interactions of aromatic groups and lipophilic interactions. A scaling function was used to penalize deviations from the ideal geometry. The docking simulations obtained were scored further using the CScore program, which is a consensus-scoring program that integrates well-known and extensively applied multiple scoring functions available with SYBYL 7.0. CScore scoring functions include root mean square deviation (RMSD) values, [13] Chemscore (scores based on a diverse set of 82 ligand-receptor complexes), [20] D_score (scores based on both electrostatic and hydrophobic contributions to the binding energy), [21] G_score (scores ligand-receptor complexes having many polar interactions), [22] FlexX_score (based on empirical functions), [14] and PMF_score (scores based on statistical ligand-receptor atom-pair interaction potentials) [23].

Hardware and software

InsightII 2000.1 and Sybyl 7.0 were used for molecular modeling on a SGI Origin 300 workstation equipped with four 600 MHz R12000 processors.

Results and discussion

Reverse transcriptase is a heterodimeric protein with a catalytic and an allosteric site and an inner core consisting of hydrophobic amino acids. This is the binding pocket for all NNRTIs. The most important amino acids involved in the hydrophobic interactions with NNRTIs are Val106, Val108, Tyr181, Tyr188, Phe227, Trp229 and Glu138 (P51 subunit), while Val179 and Lys101 may be responsible for hydrogen-bonding interactions [24, 25]. To date, numerous

Table 2 FlexX docking scores of 2-(2, 6-Dihalophenyl)-3-(substituted heteroaryl)-thiazolidin-4-ones

Comp. no.	FlexX score	G_Score	PMF_score	D_score	Chem_score	CScore (ΔG)
Pyridine analogues						
1	-12.43	-218.52	-35.66	-138.80	-30.51	5
2	-12.16	-193.12	-48.14	-121.54	-32.00	5
3	-11.58	-192.66	-49.75	-115.26	-30.16	5
4	-9.74	-138.77	-23.24	-104.79	-19.99	5
5	-10.03	-148.03	-33.04	-85.41	-19.85	5
6	-9.92	-142.03	-35.91	-84.27	-19.35	5
7	-9.80	-141.81	-23.22	-106.83	-20.18	5
8	-10.11	-127.52	-41.57	-78.82	-18.85	5
9	-9.42	-142.13	-35.91	-85.58	-19.53	5
10	-11.36	-257.01	-30.56	-164.57	-35.03	5
11	-13.37	-201.99	-44.83	-137.36	-35.26	5
12	-13.89	-217.77	-42.34	-126.80	-33.18	5
13	-7.00	-190.40	-54.98	-131.26	-31.08	5
14	-12.24	-253.21	-25.38	-157.38	-31.47	5
15	-13.04	-208.96	-45.68	-125.36	-34.10	5
16	-11.45	-193.86	-39.71	-138.83	-32.24	5
17	-9.85	-137.53	-27.11	-78.98	-19.29	5
18	-9.67	-145.36	-32.71	-83.77	-19.43	5
19	-13.27	-260.35	-22.90	-158.09	-31.72	5
20	-13.12	-204.39	-40.25	-131.92	-35.11	5
21	-13.29	-187.73	-60.36	-135.17	-29.40	5
22	-12.26	-183.39	-64.46	-545.66	-38.59	5
23	-13.40	-218.64	-42.46	-137.70	-35.81	5
24	-12.78	-224.73	-84.02	-127.22	-33.20	5
Pyrimidine analogues						
25	-11.39	-162.84	-75.33	-344.43	-32.35	5
26	-11.52	-154.10	-89.39	-325.91	-30.65	5
27	-10.06	-160.76	-46.36	-144.08	-22.24	5
28	-12.73	-174.18	-64.13	-454.24	-33.24	5
29	-12.01	-204.47	-69.28	-132.49	-33.10	5
30	-11.60	-171.94	-82.38	-117.55	-29.59	5
31	-7.88	-153.63	-31.75	-65.47	-18.34	5
32	-13.14	-89.49	-37.55	-50.58	-18.27	5
33	-13.20	-174.06	-50.17	-98.01	-21.95	5
34	-11.73	-155.05	-92.04	-545.31	-33.56	5
35	-12.61	-152.72	-59.62	-528.08	-34.29	5
36	-12.45	-169.21	-56.50	-109.67	-23.75	5
37	-11.69	-142.24	-54.50	-85.97	-19.12	5
38	-9.26	-136.91	-50.35	-74.01	-17.36	5

crystal structures of unaligned wild type and mutant HIV-RT, in complex with cognate duplex DNA substrate and different inhibitors, have been reported. With the help of crystal structures it has been possible to delineate amino acids involved in hydrophobic interactions with NNRTIs. These crystal structures provided not only insight into the interaction mechanism of the HIV-RT with the inhibitors, but also valuable clues for designing new inhibitors [26]. The new NNRTI benzimidazol-2-one scaffold was designed from the pharmacophore hypothesis and structure-based modification of the lead compound 1H,3H-thiazolo[3,4-a]benzimidazoles (TBZ) using the crystal structure of HIV-1 RT with efavirenz (PDB entry 1FK9) [26]. The consensus emerging from various NNRTIs-HIV-1RT complex studies is that all NNRTIs bind at the allosteric site and the crystal structure of a scaffold can be extrapolated to other classes of NNRTIs. Therefore, in the present study we have selected the 9-Cl-TIBO/ HIV-RT complex (PDB code-1REV) [16] for the docking study of 4-thiazolidinones.

Validation of the docking method

To ensure that the ligand orientation and the position obtained from the docking studies were likely to represent valid and reasonable binding modes of the inhibitors, the FlexX program docking parameters first had to be validated for the crystal structure used (1REV). The ligand 9-Cl-TIBO, in the conformation found in the crystal structure, was extracted and docked back into the corresponding binding pocket to determine the ability of FlexX to reproduce the orientation and position of the inhibitor observed in the crystal structure. The results of control docking showed that FlexX determined the optimal orientation of the docked inhibitor, 9-Cl-TIBO to be close to that of the original orientation found in the crystal (Fig. 1). The low RMS deviation of 0.59 Å between the docked and crystal ligand coordinates indicate very good alignment of the experimental and calculated positions, especially considering the resolution of the crystal structure (2.6 Å). As none of the structural waters are conserved among all the RT-NNRTIs crystal complexes, the docking experiments were performed without water molecules in the allosteric site. To test this procedure, 9-Cl-TIBO was docked into the binding pocket in the presence of two water molecules located within the pocket in the crystal structure. The best scoring results were in the identical relative positions to those calculated in the absence of water molecules.

Docking of 4-thiazolidinones derivatives

To study the binding modes of 4-thiazolidinones derivatives in the allosteric binding site of HIV-1 RT, intermolecular

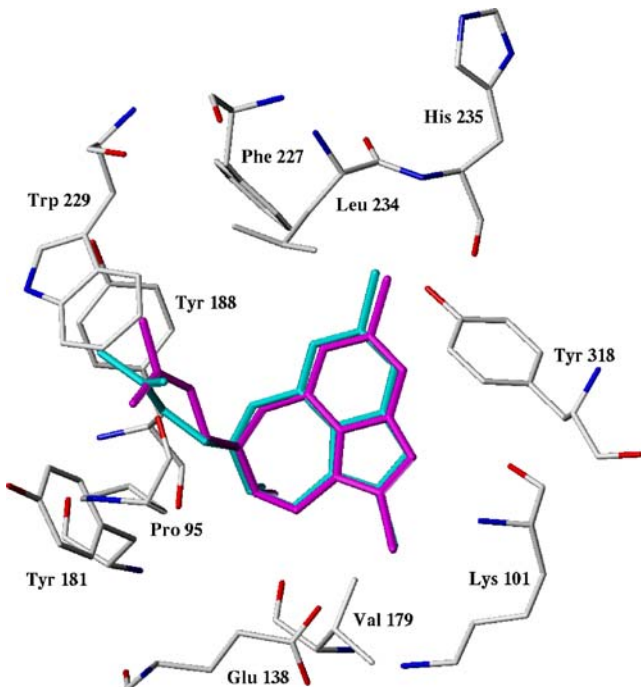


Fig. 1 Conformation of 9-Cl TIBO-Crystal structure (magenta) as compared to the docked conformation of 9-Cl-TIBO (cyan)

flexible docking simulations were performed by means of FlexX and interaction energies calculated from the docked conformations of the RT-inhibitor complexes. The docked 3D-structures of 4-thiazolidinones were compared with the X-ray crystallographic structure of 9-Cl-TIBO (Fig. 2a and b). A qualitative analysis of the binding mode found in the docked 4-thiazolidinones-RT and other NNRTIs-RT crystal complexes showed that 4-thiazolidinones could bind to RT in a butterfly-like conformation; the presence of halogen atoms at the two and six positions restricted the rotation of the phenyl ring and allowed the molecules to assume the characteristic butterfly-like conformation present in many other known NNRTIs [27]. Like 9-Cl-TIBO, (Fig. 2a and b) 4-thiazolidinones are also involved in hydrogen-bond formation with Lys 101, which was observed in the X-ray crystallographic structure of the 9-Cl-TIBO-RT complex. Thus, 4-thiazolidinones-RT complexes are primarily stabilized by extensive hydrophobic interactions as well as some specific polar ones. Following the pattern revealed by the previous studies, NNRTIs might bind to HIV-1 RT in more than one conformation; [28] 4-thiazolidinones also exhibit multiple binding conformations. Docking analyses of 4-thiazolidinones revealed that these compounds prefer one single binding position in the allosteric binding pocket, but other binding positions are also possible. Docking of pyridine analogues of 4-thiazolidinones produced two major clusters of binding conformations occupying two separate, but overlapping binding regions. Most of the top-ranking active compounds in this series (Table 1) were found to

prefer a single binding position in the allosteric pocket (Fig. 2b shows the best docked conformations of compounds **12**, **19**, **20**, **23**). Comparison of the X-ray structure of 9-Cl-TIBO with compound **12** (Fig. 2a) showed that the 3-(6-bromopyridine-2-yl) group, the 2-(2,6-difluorophenyl) ring and the CH₂-S part of the 4-thiazolidinone nucleus of the compound **12** occupy the spatial orientation corresponding to the phenyl/imidazalone rings, hydrophobic dimethylallyl and diazepine ring of the 9-Cl-TIBO, respectively. The CH₂-S moiety of 4-thiazolidinone nucleus is oriented towards a channel formed between the residues Lys101, Val179 (both from p66 subunit) and Glu138 (from the p51 subunit). The backbone-nitrogen atom of Lys101 interacts with the oxygen atom of the 4-thiazolidinone nucleus to form a hydrogen bond. The substituted pyridine ring of the compound interacts hydrophobically with residues Leu234, Tyr318 and His235 and these hydrophobic contacts contribute significantly to the stabilization of the complex. As shown in the Fig. 2, the 2,6-dihalophenyl ring is located deep inside the cavity surrounded by the residues Tyr181, Pro95, Tyr188, and Trp229, whereas moderate and less active compounds exhibit a second cluster-binding mode different from the most active compound. In this type of binding, the substituted pyridine group is oriented towards the residues Val179 and Glu138, mimicking the seven-membered benzodiazepine ring in the X-ray structure of HIV-1 RT in complex with 9-Cl-TIBO. The 2,6-dihalophenyl ring interacts hydrophobically with residues Leu234, Tyr318, His 235 and Phe227 in place of the pyridine ring in the previous binding mode of these compounds (Fig. 2c). The oxygen atom of the 4-thiazolidinone nucleus in this particular binding mode forms a hydrogen bond with the side-chain nitrogen atom of Lys103 instead of the backbone nitrogen atom of Lys101 in the other type of binding of pyridine analogues.

Docking of pyrimidine analogues of 4-thiazolidinones produced similar results. Most of the compounds in this series, including the highly active compounds, show a common type of binding (Fig. 3a and b). As shown in Fig. 3a, the 4-thiazolidinone nucleus in compound **32** is oriented towards Lys101 like the imidazole ring of 9-Cl-TIBO in the 1REV X-ray structure. The oxygen atom of the 4-thiazolidinone nucleus also forms a hydrogen bond with the backbone nitrogen atom of Lys101, as in the case of the top-ranking compounds of this series. The pyrimidine ring is oriented towards a cavity surrounded by Glu138, Tyr181, Val179 and Pro95, while the 2,6-dihalophenyl group makes hydrophobic contacts with residues Trp229, Tyr188, Leu234 and Phe229, which are necessary for the stabilization of the complex (Fig. 3b).

It is interesting to note from our docking studies that highly active compounds of pyridine and pyrimidine analogues of 4-thiazolidinones bind in different binding modes to HIV-1 RT. The possible explanation for the

different binding modes may be the difference in the hydrophobicity of two series of compounds. Replacement of an aromatic ring CH of pyridine analogues with N in the case of pyrimidine analogues leads to a decrease in the net hydrophobicity of the aromatic unit and this change may be responsible for the orientation of the substituted pyrimidine ring different from the pyridine ring, towards the pocket

formed by residues Glu138 (P51 subunit) and Val179, Pro95, Tyr181 (P66 subunit) in the protein (Fig. 3b).

Correlation between binding free energy and inhibitory activity

An important application of FlexX in structure-based drug design is to predict the binding free energies while

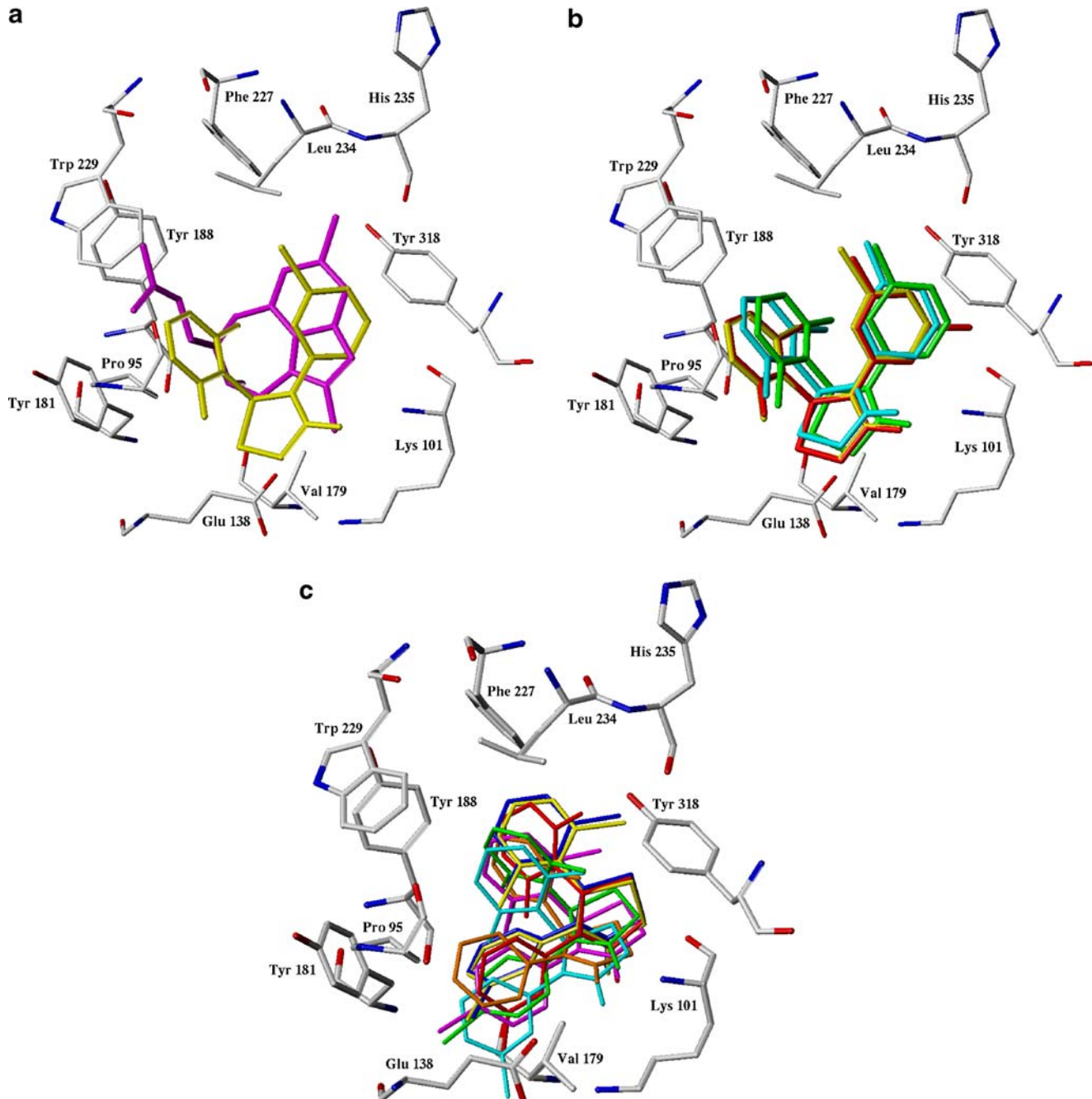


Fig. 2 Docked conformations of **a** 9-Cl-TIBO crystal structure (magenta) with best active compound **12** (yellow) **b** best four active compounds of pyridine analogues **12** (yellow), **19** (cyan), **20** (green) &

23 (red) in the binding site of HIV-1 RT **c** moderate & less active compounds of pyridine analogues **3** (orange), **5** (magenta), **9** (violet), **10** (yellow), **11** (blue), **16** (red) and **21** (cyan)

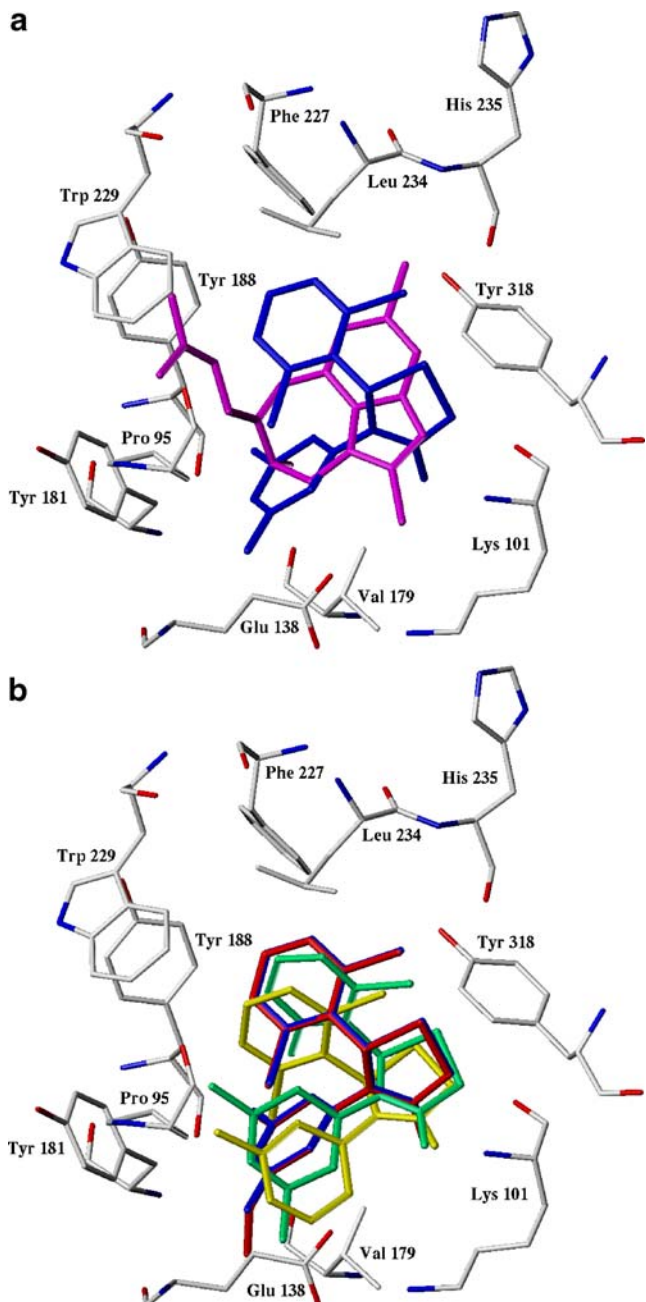


Fig. 3 Docked conformations of **a** 9-Cl-TIBO crystal structure (magenta) with best active compound of pyrimidine analogues **32** (blue) **b** best four active compounds of pyrimidine analogues **28** (yellow), **32** (blue), **33** (green blue) & **35** (red) in the binding site of HIV-1 RT

determining the binding conformation of an inhibitor with the target. The scoring reliability of FlexX was evaluated by correlating the calculated binding free energies with the experimental inhibitory activities of 4-thiazolidinones. The equation was obtained for the inhibitory activities represented as $-\log EC_{50}$ values, using the FlexX score (ΔG) as the sole descriptor variable via a linear regression, as shown

in Eq. 1 and Fig. 4. The correlation coefficient (r) for 4-thiazolidinones analogues was 0.955 for Eq. 1.

$$-\log EC_{50} = 0.167 - 0.547(0.028)\Delta G \quad n = 38, r = 0.955, Q^2 = 0.900, s = 0.286, F = 370.837 \quad (1)$$

In these regression equations, n is the number of compounds, r is the correlation coefficient, Q^2 is the cross-validated R^2 from the leave-one-out (LOO) procedure, s is the standard error of the estimate and F is the ratio between the variances of calculated and observed activities. The values given in the parentheses are the standard errors of the regression coefficients. The better correlation of binding free energies and observed activities of 4-thiazolidinones suggest that the binding of pyridine and pyrimidine analogues are appropriate in the allosteric site of HIV-1 RT.

Conclusion

In this work, molecular docking studies were carried out to explore the binding mechanism of 4-thiazolidinones inhibitors to the HIV-1 RT enzyme to enable the design of new HIV-1 RT inhibitors. Both the binding conformation of 4-thiazolidinones and their binding free energies were predicted by molecular docking. The binding models of the inhibitors demonstrate how the 4-thiazolidinone binds to HIV-1 RT. The molecular docking studies show the potential binding mode of most of the top-ranking compounds in 4-thiazolidinones to HIV-1 RT allosteric binding site. The binding free energies of these compounds to HIV-1 RT were found to have a good correlation with the

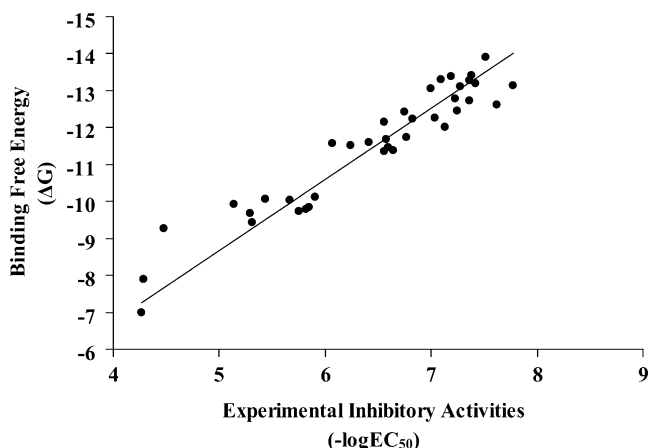


Fig. 4 Correlation between the experimental inhibitory activities ($-\log EC_{50}$) and the predicted binding free energies (ΔG kJ mol $^{-1}$) of thiazolidin-4-one analogues

experimental inhibitory activities. The most favorable binding mode of 4-thiazolidinones top-ranking compounds will be useful in designing new NNRTIs.

Acknowledgments This work was supported by Council of Scientific and Industrial Research (CSIR) funded network project CMM0017–Drug target development using in silico biology. The authors acknowledge Dr. Y.S. Prabhakar for critical reading of the manuscript. A.K. acknowledges CSIR for fellowship. C.D.R.I. communication no. of this manuscript is 6853.

References

1. De Clercq E (2005) *J Med Chem* 10:1297–1313
2. Schafer W, Fribe WG, Leinert M, Merttens A, Poll T, von der Saal W, Zilch H, Nuber H, Ziegler ML (1993) *J Med Chem* 36:726–732
3. Barreca ML, Balzarini J, Chimirri A, De Clercq E, Luca LD, Holtje MH, Holtje M, Monforte AM, Monforte P, Pannecouque C, Rao A, Zappala M (2002) *J Med Chem* 45:5410–5413
4. Rao A, Balzarini J, Carbone A, Chimirri A, De Clercq E, Monforte AM, Monforte P, Pannecouque C, Zappala M (2004) *Antiviral Res* 63:79–84
5. Prabhakar YS, Solomon VR, Rawal RK, Gupta MK, Katti SB (2004) *QSAR & Combi Sci* 23:234–244
6. Rawal RK, Solomon VR, Prabhakar YS, Katti SB, De Clercq E (2005) *Comb Chem High Throughput Screen* 8:439–443
7. Roy K, Leonard T (2005) *QSAR & Comb Sci* 24:579–592
8. Barreca ML, Balzarini J, Chimirri A, De Clercq E, Luca LD, Holtje MH, Holtje M, Monforte AM, Monforte P, Pannecouque C, Rao A, Zappala M (2002) *J Med Chem* 45:5410–5413
9. Prabhakar YS, Rawal RK, Gupta MK, Solomon VR, Katti SB (2005) *Comb Chem High Throughput Screen* 8:431–437
10. InsightII 2000.1 Program (2000) Accelrys Inc, San Diego, California
11. Sybyl 7.0 (2004) TRIPoS Inc, 1699 South Hanley Road, St. Louis, Missouri 63144, USA
12. Gasteiger J, Marsili M (1980) *Tetrahedron* 36:3219–3228
13. FlexX, version 1.13.5 (2004) BioSolveIT GmbH, Saint Augustin, Germany
14. Rarey M, Kramer B, Lengauer T, Klebe G (1996) *J Mol Biol* 261:470–489
15. Frankel EN, Waterhouse AL, Kinsella JE (1993) *Lancet* 341:1103–1104
16. Ren J, Esnouf R, Hopkins A, Ross C, Jones Y, Stammers D, Stuart D (1995) *Structure* 3:915–926
17. Ren J, Milton J, Weaver KL, Short SA, Stuart DI, Stammers DK (2000) *Structure* 8:1089–1094
18. Ren J, Esnouf R, Garman E, Somers D, Ross C, Kirby I, Keeling J, Darby G, Jones Y, Stuart D (1995) *Nat Struct Biol* 2:293–302
19. Böhm HJ (1998) *J Comput Aided Mol Des* 12:309
20. Eldridge MD, Murray CW, Auton TR, Paolini GV, Mee RP (1997) *J Comput Aided Mol Des* 11:425–445
21. Ewing TJA, Kuntz ID (1997) *J Comput Chem* 18:1175–1189
22. Jones G, Willett P, Glen RC, Leach AR, Taylor R (1997) *J Mol Biol* 267:727–748
23. Muegge I, Martin YC (1999) *J Med Chem* 42:791–804
24. Mager PP (1997) *Med Res Rev* 17:235–276
25. Tantillo C, Ding J, Jacobo-Molina A, Nanni RG, Boyer PL, Hughes SH, Pauwels R, Andries K, Janssen PA, Arnold E (1994) *J Mol Biol* 243:369–387
26. Barreca ML, Rao A, De Luca L, Zappala M, Monforte AM, Maga G, Pannecouque C, Balzarini J, De Clercq E, Chimirri A, Monforte P (2005) *J Med Chem* 48:3433–3437
27. Ding J, Das K, Moereels H, Koymans L, Andries K, Janssen PA, Hughes SH, Arnold E (1995) *Nat Struct Biol* 92:407–415
28. Das K, Levi PJ, Hughes SH, Arnold E (2005) *Prog Biophys Mol Biol* 88:209–231